

SCIENTIFIC REPORTS



OPEN

Primary macrophages and J774 cells respond differently to infection with *Mycobacterium tuberculosis*

Received: 18 October 2016

Accepted: 05 January 2017

Published: 08 February 2017

Nuria Andreu¹, Jody Phelan¹, Paola F. de Sessions², Jacqueline M. Cliff³, Taane G. Clark^{1,4} & Martin L. Hibberd^{1,2}

Macrophages play an essential role in the early immune response to *Mycobacterium tuberculosis* and are the cell type preferentially infected *in vivo*. Primary macrophages and macrophage-like cell lines are commonly used as infection models, although the physiological relevance of cell lines, particularly for host-pathogen interaction studies, is debatable. Here we use high-throughput RNA-sequencing to analyse transcriptome dynamics of two macrophage models in response to *M. tuberculosis* infection. Specifically, we study the early response of bone marrow-derived mouse macrophages and cell line J774 to infection with live and γ -irradiated (killed) *M. tuberculosis*. We show that infection with live bacilli specifically alters the expression of host genes such as *Rasd2*, *Ifit1/2/3* and *Rig-I*, whose potential roles in resistance to *M. tuberculosis* infection have not yet been investigated. In addition, the response of primary macrophages is faster and more intense than that of J774 cells in terms of number of differentially expressed genes and magnitude of induction/repression. Our results point to potentially novel processes leading to immune containment early during *M. tuberculosis* infection, and support the idea that important differences exist between primary macrophages and cell lines, which should be taken into account when choosing a macrophage model to study host-pathogen interactions.

Mycobacterium tuberculosis infection occurs by inhalation of bacilli-containing aerosols produced by patients with active pulmonary disease. In the lung, the first host cells that the bacilli encounter are the alveolar macrophages, which can identify and phagocytise *M. tuberculosis* via specific receptors such as toll-like receptors (TLRs), scavenger receptors or mannose receptor¹. These interactions lead to production of various antimicrobial peptides, cytokines and chemokines². If the pathogen is not eliminated within the alveolar macrophages, other cell types such as monocytes, dendritic cells and neutrophils are recruited and infected, leading to granuloma formation³. Once the adaptive immunity ensues, CD4⁺ T-cells arrive to the lung secreting IFN- γ that activates macrophages for efficient *M. tuberculosis* killing. Therefore, macrophages are both key effector cells in mycobacterial killing and a niche for bacterial multiplication. Understanding the mechanisms of *M. tuberculosis*-macrophage interactions is key to identify pathways central to both bacterial virulence and host immunity.

Several macrophage models have been used to study *M. tuberculosis* infection. These include primary macrophages, mainly human monocyte-derived macrophages (hMDMs) or mouse bone marrow-derived macrophages (BMDMs); and cell lines, such as the human THP-1 and U937, or the murine J774 and RAW 264.7^{4,5}. BMDMs are a useful model because they can be easily cultured and expanded to large numbers. Besides, BMDMs isolated from knockout mice enable the study of the role of specific genes/pathways during *M. tuberculosis* infection. hMDMs are a more physiologically relevant model, since they are isolated from the natural host. Additionally, hMDMs are relatively easy to obtain and differentiate *in vitro* from human blood monocytes. However, the use of human biological samples entails ethical issues, and the genetic variation that underlies the use of human donors complicates result interpretation. The use of cell lines, on the other hand, has several advantages, related mainly to the fact that they are homogenous, and very easy to propagate and maintain in the laboratory. However, cell lines derive from transformed or immortalized cells that have acquired genetic and phenotypic differences in comparison with their primary counterparts^{6–8}. Furthermore, cell lines have a tendency

¹Pathogen Molecular Biology Department, London School of Hygiene and Tropical Medicine, London, UK. ²Genome Institute of Singapore, A*STAR, Singapore. ³TB Centre and Department of Immunology and Infection, London School of Hygiene and Tropical Medicine, London, UK. ⁴Department of Infectious Disease Epidemiology, London School of Hygiene and Tropical Medicine, London, UK. Correspondence and requests for materials should be addressed to N.A. (email: nuria.andreum@gmail.com) or M.L.H. (email: Martin.Hibberd@lshtm.ac.uk)

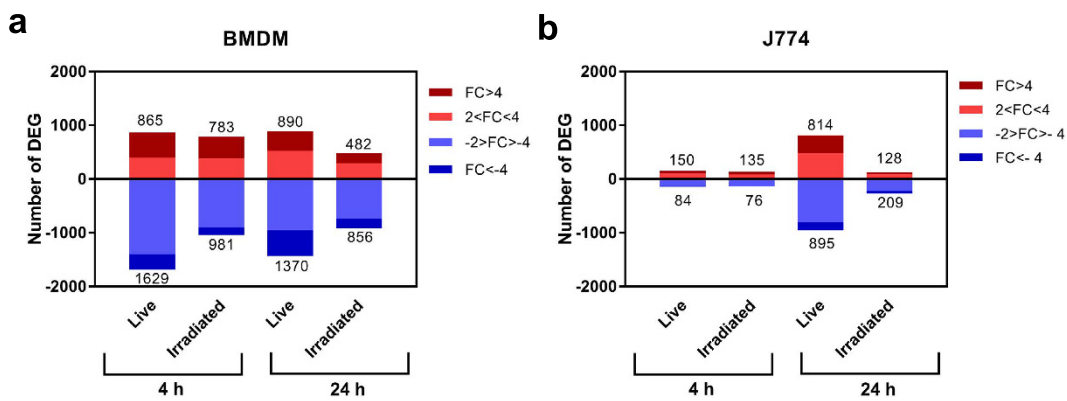


Figure 1. Number of differentially expressed genes (DEGs). (a) In BMDMs, and (b) in J774 infected with live *M. tuberculosis* or stimulated with γ -irradiated *M. tuberculosis*, relative to their time-matched uninfected controls, at 4 and 24 hpi (FDR < 0.05). The colour shading indicates the fold change in gene expression. The number of DEGs is indicated.

to be genetically unstable, with hybrid phenotypes and possibly atypical signalling mechanisms. Therefore, the question remains on whether cell lines are physiologically relevant systems, particularly for host-pathogen interaction studies.

Previous comparisons of macrophage infection models for *M. tuberculosis* have focused on certain phenotypic traits such as intracellular growth, cytokine production, or phagosome characteristics^{5,9,10}. Jordao and collaborators found that *Mycobacterium bovis* grows more efficiently in hMDMs than in J774 over a 7-day time course, even though both types of macrophages can restrict growth during the first 24 hours of infection through a mechanism involving phagosome acidification and nitric oxide production⁹. Mendoza and collaborators compared *M. tuberculosis*, *M. bovis* and *M. bovis* BCG infection of hMDMs, THP-1 and U937, and found that U937 has a lower phagocytic capacity than the other two. They also compared production of nitrite, TNF- α and IL-12 in resting and IFN- γ activated macrophages, and found that THP-1 resembles more closely hMDMs¹⁰.

Here we focus on two mouse macrophage models that are widely used to study *M. tuberculosis* infection: BMDMs (primary macrophages) and J774A.1 (a cell line, hereafter referred to as "J774" for simplicity). We conduct an in depth analysis of their transcriptomic response to infection with live *M. tuberculosis* and stimulation with γ -irradiated (killed) *M. tuberculosis*. We find that BMDMs respond very strongly to infection whereas the response of J774 is delayed and more discreet both in terms of number of differentially expressed genes and magnitude of induction/repression. Furthermore, we identify macrophage genes whose possible function in resistance to *M. tuberculosis* infection has not yet been investigated.

Results

Global transcriptome profiles. BMDMs and J774 macrophages were either infected with live *M. tuberculosis* H37Rv or stimulated with γ -irradiated (killed) *M. tuberculosis* H37Rv for 4 hours. Total RNA was isolated at 4 and 24 hours post-infection (hpi), and CFUs were determined by plating dilutions of lysed macrophages. At 24 hpi, a 0.34 log and a 0.2 log decrease in CFUs was observed in BMDMs and J774, respectively (see Supplementary Fig. S1). Total RNA was used to construct individually barcoded, strand-specific RNA-seq libraries after depletion of ribosomal and mitochondrial RNA, and the libraries were sequenced on an Illumina® HiSeq™ 2000 apparatus.

To investigate general trends in the data, principal component analysis (PCA) was carried out (see Supplementary Fig. S2). PCA confirmed no outlier samples and showed separate grouping of uninfected macrophages (controls), and macrophages infected with live bacteria or stimulated with dead bacteria. The transcriptome profiles of BMDMs infected with live bacteria or stimulated with dead bacteria were similar to each other at 4 hpi and became more distinct (from each other and especially from the 4-hpi samples) at 24 hpi. For the J774 cells, PCA showed grouping of the transcriptomes of cells infected with live bacteria or stimulated with dead bacteria at 4 hpi and those of cells stimulated with dead bacteria at 24 hpi; that is, in the case of J774 cells, the 24-hpi transcriptome of cells stimulated with dead bacteria was not clearly different from the 4-hpi transcriptomes.

In addition, the transcriptome of BMDMs uninfected controls (but not that of J774 uninfected cells) changed considerably from 4 hpi to 24 hpi (Supplementary Fig. S2, and Supplementary Data S1). That is, considerable changes occurred in the transcriptome of uninfected BMDMs while they were maintained in culture, emphasising the need to process a matched non-infected control for each time point when using primary macrophages. These differences in the transcriptome of *in vitro* grown primary macrophages over time had been previously observed by others both with murine macrophages¹¹ and human macrophages¹².

Differences between the transcriptional responses of BMDMs and J774 cells. Differential expression analysis demonstrated a clear response of *M. tuberculosis*-infected BMDMs as early as 4 hpi. A total of 2,494 significantly differentially expressed genes (DEGs) with an absolute fold change (FC) greater than 2 ($|FC| > 2$ or $|\text{Log}_2 \text{FC}| > 1$) were detected at 4 hpi in BMDMs infected with live bacteria compared to uninfected BMDMs (FDR < 0.05) (Fig. 1a, and Supplementary Data S2). By contrast, only 234 DEGs were detected for J774 when

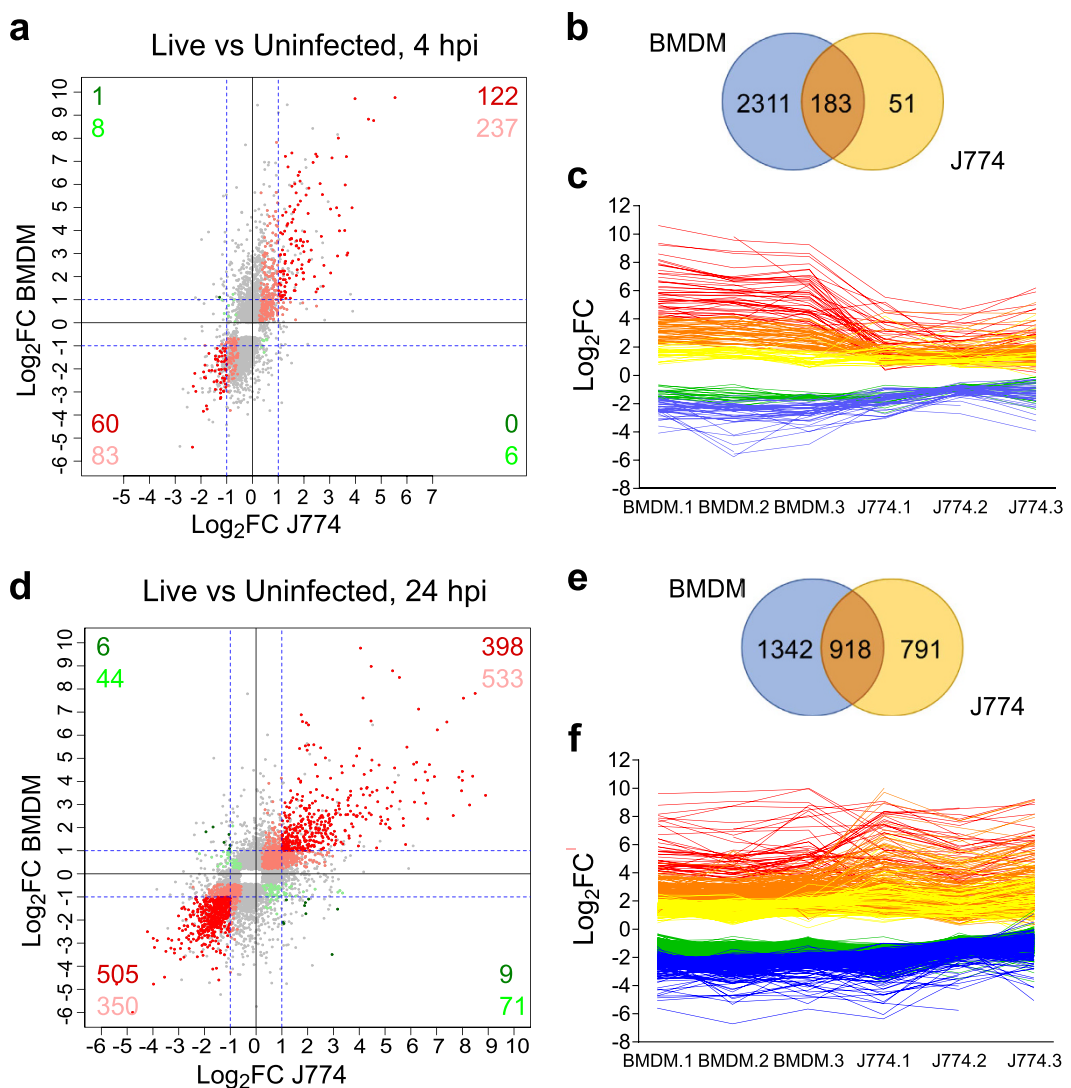


Figure 2. Comparison of the response of BMDMs and J774 to infection with live *M. tuberculosis*.

Scatterplots comparing the \log_2 fold change (FC) of all the differentially expressed genes (DEGs) in BMDMs and J774 at 4 hpi (a) and 24 hpi (d). Grey dots represent genes differentially expressed in one macrophage type only. Points in shades of red represent genes differentially expressed in both data sets in the same direction. Points in shades of green represent genes differentially expressed in opposite direction. Those showing $FC < |2|$ in either/both condition(s) are shown in light colour and those with $FC > |2|$ in both conditions are shown in dark. The number of genes are indicated for each quadrant. (b) and (e) Venn diagrams comparing DEGs in BMDMs and J774 at 4 hpi and 24 hpi, respectively. (c) and (f) Line graphs showing the variation of the \log_2 FC for each DEG in common between BMDMs and J774 at 4 hpi (c) and 24 hpi (f). Lines are coloured according to the \log_2 FC in BMDMs (\log_2 FC > 4 red, $2 < \log_2$ FC < 4 orange, $1 < \log_2$ FC < 2 yellow, $-1 > \log_2$ FC > -2 green, $-2 > \log_2$ FC blue).

comparing uninfected vs infected with live bacteria ($FDR < 0.05$, $|FC| > 2$, Fig. 1b, and Supplementary Data S2). Of these 234 DEGs, 183 were also differentially expressed in BMDMs (Fig. 2a and b, and Supplementary Data S3), representing 78% and 7.4% of the DEGs in J774 and BMDMs, respectively. Furthermore, 182 of the 183 common DEGs were differentially expressed in the same direction, with 122 upregulated (top right quadrant of the scatter plot in Fig. 2a), and 60 downregulated (bottom left quadrant, Fig. 2a). However, the absolute fold change in expression of 136 (74.3%) of the 183 common DEGs was higher in BMDMs than in J774 (Fig. 2c). This was a general trend, with a \log_2 FC range between -5.39 and $+9.76$ in BMDMs, whereas in J774 it was narrower, between -2.33 and $+5.54$.

The number of DEGs in J774 (but not in BMDMs) increased considerably from 4 to 24 hpi, but was still lower than the number of DEGs in BMDMs (Fig. 1, and Supplementary Data S2). 918 genes with a $|FC| > 2$ were differentially expressed at 24 hpi in both BMDMs and J774 cells (Fig. 2d and e, and Supplementary Data S3). These represent 41% and 54% of the total DEGs at 24 hpi, respectively. Of these 918 common DEGs, 903 were differentially expressed in the same direction, with 398 upregulated (top right quadrant of the scatter plot), and 505

downregulated (bottom left quadrant, Fig. 2d). At 24 hpi, the level of response was more similar between the two types of cells, with only 55% of the common DEGs presenting a Log₂FC significantly different (Fig. 2f). Overall, the global level of induction/repression was similar at 24 hpi in both types of macrophages ranging from -6.00 to +9.77 in BMDMs, and -5.41 to +9.84 in J774. Of note, 104 of the common DEGs detected at 4 hpi were also differentially expressed in both cell types at 24 hpi, including most of the top differentially expressed ones.

Core response of murine macrophages to infection with live *M. tuberculosis*. A more detailed examination of the genes differentially expressed in both J774 and BMDMs highlighted many genes previously described as important during *M. tuberculosis* infection (Supplementary Data S3). These include receptors for the recognition and phagocytosis of *M. tuberculosis*, such as the C-type lectin receptor Mincle (*Clec4e*) and the class A scavenger receptor MARCO, both of which were induced; the mannose receptor (*Mcr1*), that was repressed; and the cytosolic receptors *Nod1* and *Nod2*, and *Tlr2*, induced. The products of other shared induced genes are involved in the activation and recruitment of antimicrobial mechanisms, like the CD40 receptor that activates antimicrobial mechanisms in infected macrophages upon interaction with ligand CD40L in T-cells¹³; several IFN-inducible GTPases such as *Gbp6*, *Gbp7*, *Irgm1* (*Lrg-47*) and *Irgm2*, which confer cell-autonomous immunity to mycobacterial infection^{14,15}; *Isg15*, which induces IFN- γ -production in lymphocytes¹⁶; *Irg1*, with bactericidal properties against *M. tuberculosis* through various mechanisms including inhibition of its isocitrate lyase^{17–19}; *Il1b*, which stimulates antimycobacterial immunity in macrophages^{20,21}, and caspase-1 (*Casp1*), required for processing of pro-IL-1 β into its active form²². *Mmp9* and *Ccl5* (*Rantes*), associated with recruitment of monocytes and macrophages during granuloma formation^{23,24}, and the neutrophil and lymphocyte-recruiting chemokines *Cxcl2*, *Cxcl10* and *Cxcl11* were also induced; as were the pro-apoptosis genes *Ptgs2* (*Cox2*) and *Ptges* (*Pges*), while the pro-necrosis gene *Alox5* was repressed.

Several interferon-stimulated genes (ISGs) were also highly induced, such as *Rasd2* (*Viperin*), *Mx1*, *Mx2*, *Ifit1*, *Ifit2*, *Ifit3*, *Ifi205*, *Apol9a*, and *Apol9b*, all with known antimicrobial functions^{25–27} but without a known function during *M. tuberculosis* infection. Interestingly, the gene encoding RIG-I (*Ddx58*) was also induced. RIG-I is a pattern recognition receptor involved in viral RNA recognition, critical for the host antiviral response. The top downregulated genes included *Rtn4rl1*; the apoptosis activator *Bmg*; the receptor *Epha2*, whose absence is associated with a reduced bacterial load during the chronic phase of *M. tuberculosis* infection in mice²⁸; *Gpr34*, whose deficiency in mice has been associated with an altered immune response^{29,30}; the chemokine *Ccl24*; and the scavenger receptor *Fcrls*.

Pathway analysis of DEGs in macrophages infected with live *M. tuberculosis*. To gain insight into the cellular and molecular functions of the *M. tuberculosis*-induced host genes, DEGs in macrophages infected with live bacteria were subjected to pathway analysis using QIAGEN's Ingenuity® Pathway Analysis (IPA®). A full list of all the enriched pathways for each condition can be found online in the Supplementary Data S4. Comparison analysis was used to visualise the results across all four conditions.

The top enriched pathways are shown in Fig. 3. Pathways are ranked according to the enrichment score (Fisher's exact test *P*-value, Fig. 3a), and to the Z-score which predicts activation or inhibition of the pathways by comparing observed and predicted regulation patterns (Fig. 3b). The same pathways were enriched in BMDMs and J774 although with different scores. For most pathways, the enrichment score and the Z-score was higher in BMDMs than in J774, particularly at 4 hpi, reflecting the stronger response in this type of macrophages early after the infection (Fig. 3).

TREM1 (triggering receptor expressed on myeloid cells 1) was one of the most significantly enriched pathways, with a high activation score in all conditions. TREM1 is a DAP12-associated receptor that plays an essential role in innate immunity by fine-tuning the inflammatory response³¹. In our dataset, many of the genes encoding cytokines and chemokines whose expression and secretion is induced by TREM1 activation, as well as several genes encoding cell surface proteins, were upregulated (see Supplementary Fig. S3). In addition to regulating the innate immune response, TREM1 modulates the adaptive immune response by inhibiting the regulators SIGIRR, which downregulates the Th1 response, and ST2, which enhances the Th2 response³². Both SIGIRR and ST2 were downregulated in our dataset.

Several pathways involved in bacterial recognition by host cells were also activated such as “Activation of IRF by cytosolic pattern recognition receptors”, “Role of RIG-1 like receptors in antiviral innate immunity”, “Toll-like receptor signalling”, or the more general pathway “Role of pattern recognition receptors in recognition of bacteria and virus” which includes TLR, NLR, RIG and complement receptors (Fig. 3).

Only a few pathways had a negative Z-score (inhibition), including PPAR signalling, LXR/RXR activation, and antioxidant action of vitamin C (Fig. 3b). Of these, PPAR signalling had the highest enrichment score. The PPAR (proliferator-activated receptor) family are ligand-activated transcriptional regulators activated by fatty acids and their derivatives. They regulate the expression of genes involved in lipid metabolism, and their function is suppressed by cytokines such as IL-1 and TNF- α .

Cell type-specific response to *M. tuberculosis* infection. A full list of the genes differentially expressed exclusively in one of the two macrophage models at a particular time point can be found online (Supplementary Data S3). Some of the genes induced exclusively in BMDMs included the chemokines *Cxcl1*, *Cxcl3* and *Cxcl9*, the cytokines *Il1a*, *Il6*, and *Il12b*; *Rasgrp1*, which participates in T cell activation; *Mmp14*, which regulates monocyte migration and collagen destruction in tuberculosis³³; *Serpinb2*, also known as plasminogen activator inhibitor type 2 (*Pai-2*), a major product of activated monocytes/macrophages which has been linked to regulation of Th1 responses³⁴; and *Fpr2*, a recently described pathogen recognition receptor that recognizes bacterial signal peptides and triggers classical innate immune responses, such as intracellular Ca²⁺ mobilization, generation of reactive oxygen species, release of metallopeptidase, and chemotactic cell migration³⁵. *Hes1*,

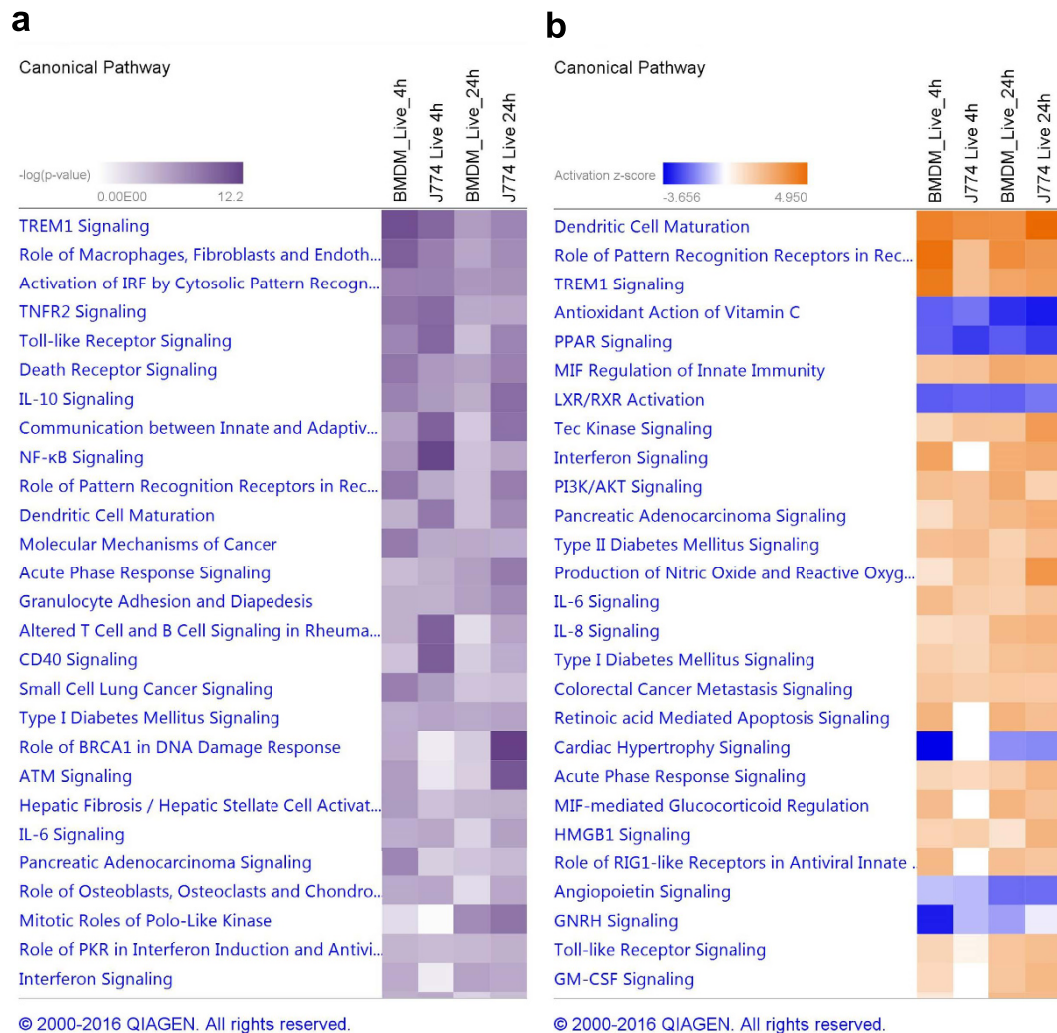


Figure 3. Top enriched pathways in macrophages infected with live *M. tuberculosis*. Data were analysed through the use of QIAGEN’s Ingenuity® Pathway Analysis (IPA®, QIAGEN Redwood City, www.qiagen.com/ingenuity). Pathways are ranked according to (a) the enrichment score (Fisher’s exact test *P*-value), and (b) the *Z*-score that predicts activation/repression.

a Notch target gene that suppress TLR-triggered pro-inflammatory cytokine production³⁶, was one of the most downregulated genes in BMDMs.

Among the top induced genes solely in J774 there was *Nos2*, highly induced at 24 hpi; *Rab15*, involved in endocytic recycling^{37,38}; the gene encoding for the laminin subunit gamma-2 (*Lamc2*); *Kdm6b* also known as *Jmjd3*, a lysine-specific demethylase that modulates pro-inflammatory responses in macrophages³⁹ and has been recently implicated in foamy macrophage formation during mycobacterial infection infection⁴⁰; the IFN-inducible GTPase *Gbp1*; and *Il23a*, required for long term control of *M. tuberculosis*⁴¹ (Supplementary Data S3). *Tlr5* and *Thr8* were some of the downregulated genes exclusively in J774, together with *Il10* that was repressed at 24 hpi in J774 while it was induced in BMDMs at 4 hpi.

Pathway analysis did not reveal any cell-specific pathways, although at 4 hpi some pathways were enriched exclusively in BMDMs, which is not unexpected given the modest response exhibited by J774 cells at this early time point (Fig. 3). Some of the pathways induced in BMDMs at 4 hpi but not in J774 until 24 hpi were “Interferon signalling” and “Role of RIG1-like receptors in antiviral innate immunity”.

Immune response of macrophages to stimulation with γ-irradiated *M. tuberculosis*. To study if the differences detected between both cell types were due to differences in the response to either phagocytosis or infection, the transcriptome of macrophages stimulated with dead (γ-irradiated) *M. tuberculosis* was also analysed by RNA-seq. Similar to what was observed when infecting with live bacteria, differential expression analysis of macrophages stimulated with dead bacteria compared to uninfected macrophages at 4 hpi showed a stronger response in BMDMs (1,764 DEGs) than in J774 (211 DEGs) (Fig. 1). At 24 hpi the number of DEGs slightly decreased in BMDMs (1,338 DEGs) and increased in J774 (337 DEGs). Moreover, the magnitude of regulation in macrophages infected with live bacteria and stimulated with dead bacteria was similar in BMDMs at both time points, and in J774 at 4 hpi, but lower in J774 stimulated with dead bacteria at 24 hpi. Specifically, the Log₂FC in

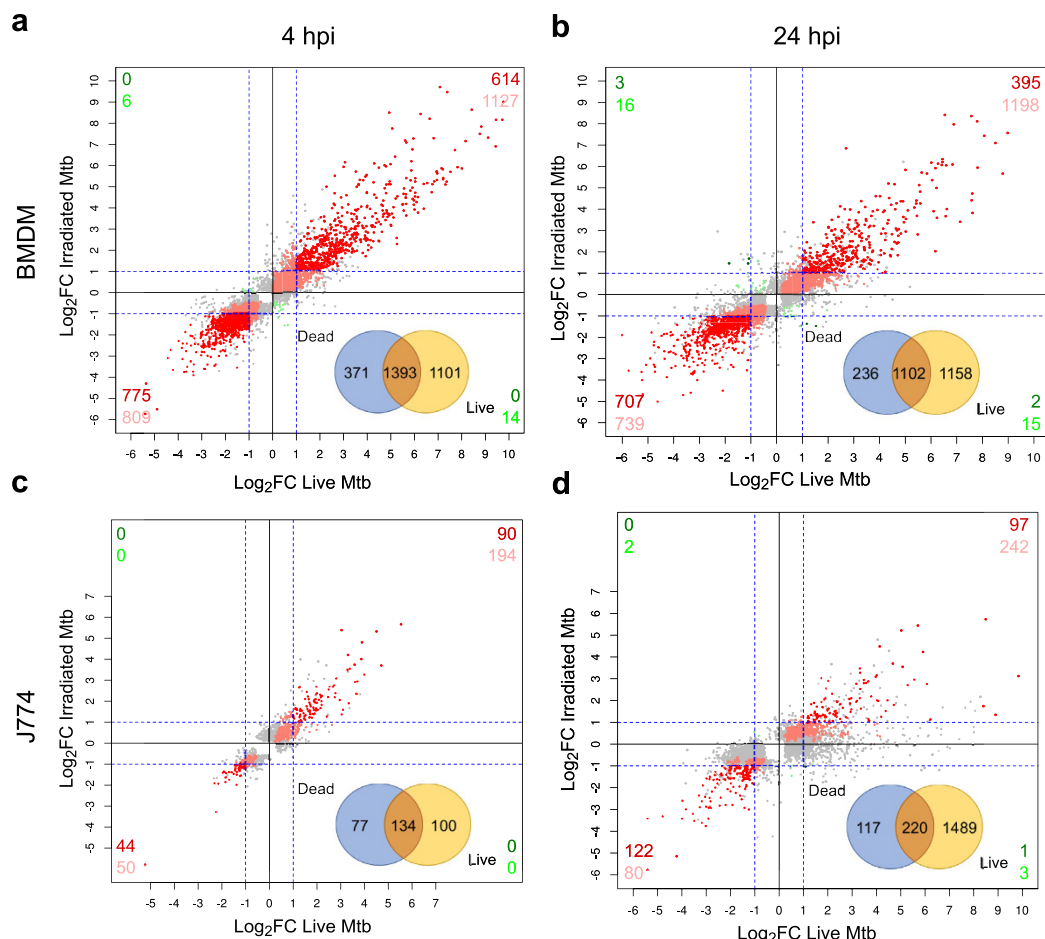
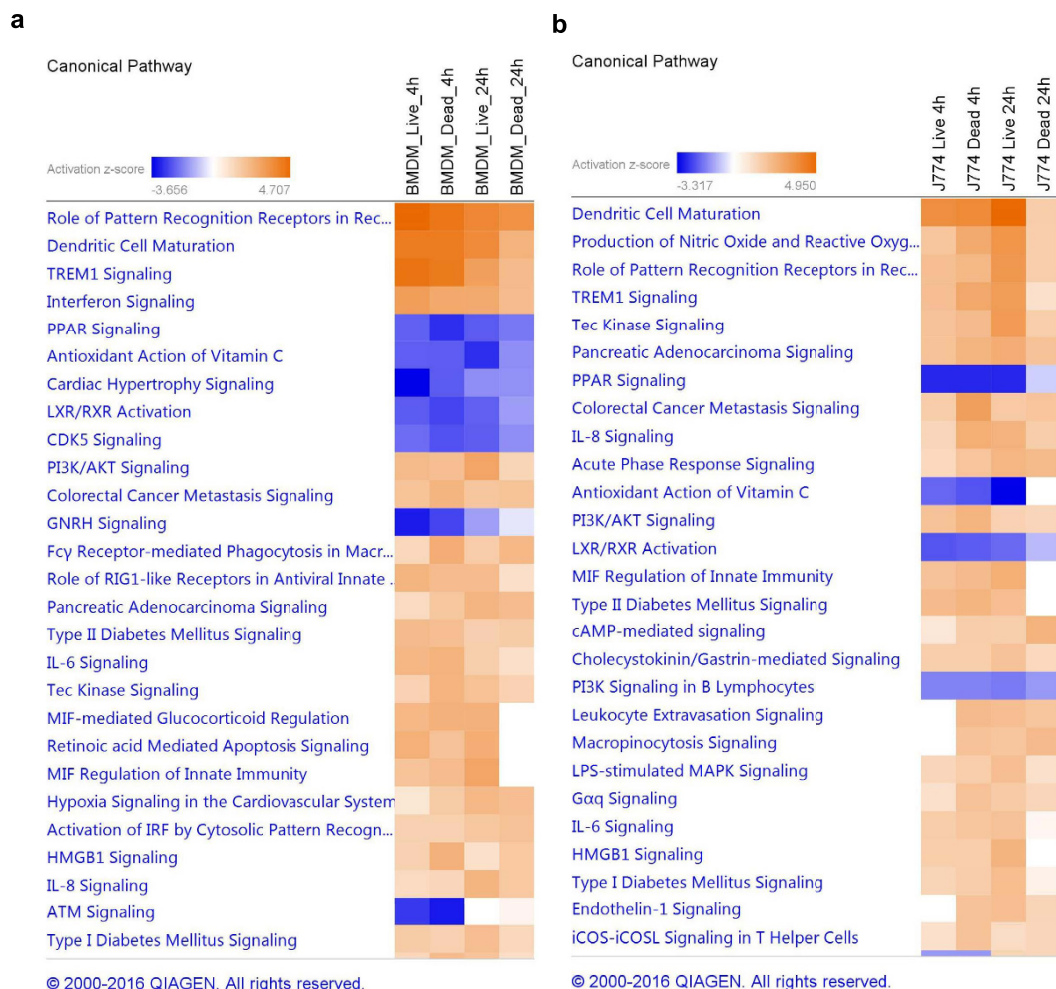


Figure 4. Comparison of the response of BMDMs and J774 to infection with live bacteria and stimulation with dead *M. tuberculosis*. Scatterplots comparing the \log_2 fold change (FC) of all the differentially expressed genes (DEGs) in BMDMs at 4 hpi (a) and 24 hpi (b), and J774 at 4 hpi (c) and 24 hpi (d). Grey dots represent genes differentially expressed in one condition only. Points in shades of red represent genes differentially expressed in both data sets in the same direction. Points in shades of green represent genes differentially expressed in opposite direction. Those showing $FC < |2|$ in either/both condition(s) are shown in light colour and those with $FC > |2|$ in both conditions are shown in dark. The number of genes are indicated for each quadrant. A Venn diagram showing the number of DEGs in macrophages infected with live bacteria and/or stimulated with dead bacteria is shown for each macrophage type and time point.

gene expression ranged from -5.73 to $+9.71$ and from -5.00 to $+9.98$ in BMDMs at 4 hpi and 24 hpi, respectively, and from -3.28 to $+5.66$ and -5.15 to $+5.73$ in J774. A full list of all the DEGs ($|FC| > 2$) can be found online in the Supplementary Data S2.

Pairwise comparisons of DEGs in macrophages stimulated with dead bacteria or infected with live bacteria showed a marked overlap, particularly in BMDM. 79% and 82% of the DEGs in BMDMs stimulated with dead bacteria were also differentially expressed in BMDMs infected with live bacteria at 4 hpi and 24 hpi, respectively (Fig. 4a and b). These correspond to 58% and 48% of the DEGs in BMDMs infected with live bacteria, respectively. Similarly, 64% and 65% of the DEGs in J774 stimulated with dead bacteria were also differentially expressed in J774 infected with live bacteria at 4 hpi and 24 hpi, respectively (Fig. 4c and d). These correspond to 57% of the DEGs in J774 infected with live bacteria at 4 hpi, but only 13% of the DEGs in J774 infected with live bacteria at 24 hpi (Fig. 4c and d). This reflects the substantial difference in the total number of DEGs between the two conditions in J774 at 24 hpi (Fig. 1b). Nevertheless, in all four comparisons virtually all the common genes were differentially expressed in the same direction and magnitude (Fig. 4). Consequently, pathway analysis results were similar in macrophages stimulated with dead bacteria and macrophages infected with live bacteria, and all the pathways had the same direction of activation/inhibition prediction (Fig. 5). As expected, the degree of activation/inhibition (Z-score absolute value) was similar in macrophages stimulated with dead bacteria or infected with live bacteria at 4 hpi but lower in macrophages stimulated with dead bacteria at 24 hpi. Overall, these results indicate that the differences detected in the transcriptomic responses between the two cell types occur even just upon phagocytosis of dead *M. tuberculosis*.



© 2000-2016 QIAGEN. All rights reserved.

© 2000-2016 QIAGEN. All rights reserved.

Figure 5. Top enriched pathways in macrophages infected with live bacteria and stimulated with dead *M. tuberculosis*. (a) BMDMs, and (b) J774 cells. Data were analysed through the use of QIAGEN's Ingenuity® Pathway Analysis (IPA®, QIAGEN Redwood City, www.qiagen.com/ingenuity). Pathways are ranked according to the Z-score that predicts activation/repression.

Discussion

Macrophages play an essential role in the early immune response against *M. tuberculosis* and are the cell type preferentially infected *in vivo*. The failure of an appropriate macrophage response is critical for the establishment of infection and progression of the disease. *M. tuberculosis* has evolved multiple evasion mechanisms in order to survive and grow inside macrophages. To study the antimicrobial response of macrophages and the evasion mechanisms of *M. tuberculosis* both primary macrophages and cell lines are commonly used. BMDMs are a popular model because they are easy to obtain, and can be sourced from a variety of specific genetic backgrounds. Likewise, the cell line J774 is frequently used since it is readily available, and no animals are involved, which results in a reduction in the number of animals used in research. In the present study, we compare the transcriptomic response of BMDMs and the macrophage-like cell line J774 to infection with *M. tuberculosis* H37Rv by using high-throughput RNA-seq.

We have found that BMDMs respond very strongly to infection whereas the response of J774 to *M. tuberculosis* infection is weaker both in terms of number of DEGs and magnitude of induction/repression, at least during the early time points of the infection. A strong host response similar to that obtained in BMDMs has been previously observed using microarrays in murine BMDMs infected with live *M. tuberculosis* strains CDC1551 and HN878 by Koo *et al.*⁴². A high number of DEGs were detected early in the infection (6 hpi) followed by a decrease in the number of DEGs at 24 hpi⁴². Other studies using human or bovine MDMs have reported a more modest response in the first hours of the infection followed by a marked increase in the amount of DEGs detected at around 18–24 hpi, similar to what we have observed in the J774 cell line^{43–45}. Interestingly, previous work has shown that infection with *Yersinia enterocolitica* results in a higher number of upregulated genes in BMDMs than in J774 cells^{46,47}. This seems to be due to a higher susceptibility of J774 to inhibition by specific anti-host effector proteins from *Y. enterocolitica* that interfere with host signalling pathways⁴⁷. Whether a similar scenario occurs upon infection with *M. tuberculosis* would be difficult to establish considering the multifactorial nature of its virulence. An additional explanation would be that J774, which derive from a lymphoma, are already in a relatively

activated state with enhanced glycolysis, which may have contributed to the reduced response observed at 4 hpi compared to the more naïve BMDM.

It is important to note that the BMDMs used in the present study were obtained from C57BL/6 mice, an extensively studied mouse strain from which most knockout mutants derive, whereas the J774 cell line derives from Balb/c mice. Some differences have been described in the immune response of these two mouse strains to *M. tuberculosis* infection and BCG vaccination *in vivo*, entailing mainly a greater early innate response (measured by production of IL-12, IFN- γ , TNF- α , MCP-1 and neutrophil influx) but a suppressed Th1 response in Balb/c compared to C57BL/6^{48,49}. However, both strains control the infection similarly and have been classified as resistant to *M. tuberculosis* infection in comparison to other more susceptible mouse strains⁵⁰. Besides, they both mount a comparable protective immunity upon vaccination with BCG⁵¹. Additionally, their BMDMs respond very similarly to *M. tuberculosis* infection *in vitro*^{52,53}. However, we cannot rule out that the differences we have observed are the result of both the different origin of the cells and of them being primary cells and a cell line.

Except for the more modest response of J774 cells, the type of response of both macrophage types to *M. tuberculosis* infection was quite similar in terms of DEGs and pathways enriched, particularly at 24 hpi. Importantly, several previously described antimycobacterial mechanisms were induced in our dataset such as *Irgm1* (*Lrg-47*) and *Irgm2*, or *Isg15*. Many other ISGs with known antimicrobial function were also induced, such as *Rasd2* (*Viperin*) or *Ifit1/2/3*. To the best of our knowledge, a specific role for many of these genes in *M. tuberculosis* infection has not been described. Therefore, the study of their involvement in the defence against *M. tuberculosis* is worth exploring.

An interesting pathway that was highly induced in both macrophages was TREM1. TREM1 has been shown to regulate the host response at an early stage during infection of various pathogens such as *Streptococcus pneumoniae*⁵⁴, *Klebsiella pneumoniae*⁵⁵, and *Streptococcus suis*⁵⁶, and it is induced in humans during active tuberculosis⁵⁷. Although the ligand of TREM1 is unknown, it has been speculated that pathogen-associated molecular patterns could directly activate it³¹, therefore it would be interesting to study if any of the *M. tuberculosis* cell wall components is a ligand for this receptor.

The PPAR signalling pathway was repressed. Current evidence indicates that mycobacterial infection causes a time-dependent increase in PPAR γ expression through a macrophage mannose receptor-dependent pathway⁵⁸. This induction results in increased lipid droplet formation and down-modulation of the macrophage response, suggesting that PPAR γ expression might aid the mycobacteria in circumventing the host response. In fact, knockdown of PPAR γ in human macrophages has been shown to result in an increase in TNF production and a decrease in *M. tuberculosis* growth at 24 hpi⁵⁸. The inhibition of this pathway together with the antimicrobial mechanisms previously mentioned could explain the control of *M. tuberculosis* growth by the macrophage at this early stage of the infection^{9,59–61}. PPAR is a well-known pathway associated with diabetes⁶². Interestingly there is now a recognised connection between diabetes and tuberculosis⁶³, although the mechanisms leading to this interaction are still unclear^{64,65}. However, with the PPAR γ pathway common between these diseases, it could be worthwhile to explore this connection in more detail.

It has been recently recognised that *M. tuberculosis* derived-products reach the cytosol early during infection via the formation of pores in the phagosomal membrane in an ESX1-dependent process⁶⁶. Both *M. tuberculosis* DNA and cyclic-di-adenosine monophosphate (c-di-AMP) are recognized by cytosolic receptors triggering production of type I IFN, ISGs and pro-inflammatory cytokines such as IL-1 β through the (cGAS)-STING-TBK1-IRF3 and AIM2-NLRP3-IL-1 β signalling pathways^{67,68}. Surprisingly, the STING/TBK1 axis was not differentially expressed in our dataset but the genes for other DNA sensors such as *Dai* (*Zbp*) and *Ifi204*, and for RNA sensors such as RIG-I (*Ddx58*), LGP2 (*Dhx58*), and MDA5 (*Ifih1*) were induced, as were the downstream transcription factors NF- κ B, IRF7, IRF9, STAT1 and STAT2, the effectors IFN β and IL-1 β , and many of the ISGs, particularly in BMDMs (at both time points, and either upon infection with live bacteria or stimulation with dead bacteria), but only marginally in J774 infected with live bacteria at 24 hpi. The importance of cytosolic nucleic acid receptors in the antimicrobial defence against bacteria has been increasingly recognized^{69,70}. The relevance of the activation of these signalling pathways during *M. tuberculosis* infection and the origin of the DNA/RNA that they would sense deserves further investigation.

The similarity in the host response in macrophages infected with live bacteria or stimulated with γ -irradiated bacteria at this early stage of the infection is not surprising if we consider that, contrary to what happens with heat-killing, inactivation by γ -irradiation preserves cell integrity⁷¹. Therefore, the same pathogen associated molecular patterns (PAMPs) are recognized by the cell's pattern recognition receptors (PRRs) leading to the same downstream signalling pathways being activated⁷². Furthermore, several studies have shown that cells inactivated by γ -irradiation are still metabolically active and *de novo* transcription and translation still occurs^{71,73}. Consequently, it would be safe to speculate that during macrophage stimulation with γ -irradiated *M. tuberculosis* the early host-pathogen interactions are conserved. This would most likely include activation of the cytosolic surveillance pathway through ESX-1-mediated cytosolic access, in the same way that γ -irradiated *Francisella tularensis* is able to escape the endosome into the cytoplasm⁷⁴. In fact, many of the hallmark genes of the cytosolic surveillance pathway were highly induced in BMDMs stimulated with dead bacteria. The induction was particularly high at 4 hpi and it decreased at 24 hpi ($\text{Log}_2\text{FC} \approx 1–2$) while it was still high in macrophages infected with live bacteria ($\text{Log}_2\text{FC} \approx 3–4$). It is likely that, at later time points, macrophages stimulated with inactivated bacteria incapable of replication can digest the bacteria and slowly shutdown their response. This would also explain the low number of DEGs at 24 hpi in macrophages stimulated with dead bacteria compared to macrophages infected with live bacteria.

In conclusion, comparison of the response of bone marrow-derived primary macrophages and the macrophage-like cell line J774 has highlighted differences in the timing and strength of the response. These differences should be taken into account when using a macrophage model for the study of host-pathogen interactions. Furthermore, the use of high-throughput RNA-seq has allowed delineation of the macrophage transcriptomic

response to *M. tuberculosis* infection in great depth, identifying genes whose function in resistance to *M. tuberculosis* infection has not yet been investigated. These findings point to potentially novel processes leading to immune containment early in the infection.

Methods

Bacterial strains, growth, and γ -irradiation conditions. *M. tuberculosis* H37Rv (ATCC 27294) was grown in Middlebrook 7H9 supplemented with 0.05% Tween 80 and 10% albumin-dextrose-catalase (ADC), or on 7H11 agar supplemented with 10% oleic acid-albumin-dextrose-catalase (OADC) at 37°C. Log-phase cultures were collected, washed twice with PBS + 0.05% Tween80 (PBS-T), and resuspended in Dulbecco's PBS (DPBS) before measuring the absorbance at 600 nm and plating CFUs. 1 ml aliquots in 2 ml tubes were irradiated at room temperature at 2.5×10^4 Gy using a Cs¹³⁷ irradiator. Inactivation of the bacteria was verified by inoculating 100 μ l in liquid and solid media and incubating for 6 weeks.

Infection of BMDMs and J774 cells with *M. tuberculosis*. Animal protocols were performed in accordance with the Animals (Scientific Procedures) Act of 1986 and were approved by the animal welfare and ethical review board of the London School of Hygiene and Tropical Medicine. Bone marrow cells were flushed from the femur and tibia of 8 to 10 week old female C57BL/6 mice and differentiated into macrophages for 7 days in DMEM (Sigma) supplemented with 10% heat-inactivated fetal bovine serum (Biosera) and 20 ng/ml M-CSF (PeproTech). On day 4, cells were fed with an additional 10 ml of media. After 7 days in culture, cells were washed with DPBS and 5×10^6 cells were seeded into 25 cm² tissue culture flasks.

J774A.1 cells obtained from the ATCC (TIB-67) were cultured in DMEM (Sigma) supplemented with 10% heat-inactivated fetal bovine serum (Biosera) and 5×10^6 cells were seeded into 25 cm² tissue culture flasks for infection.

Mid-log phase *M. tuberculosis* were washed twice with PBS-T, once with DPBS, diluted in DMEM and added to either BMDMs or J774 cells at a concentration of $\sim 2.5 \times 10^7$ CFU/flask (MOI of 5). After 4 h of infection at 37°C in 5% CO₂, macrophages were treated with 200 mg/l amikacin for 1 h and washed twice with DPBS to eliminate any extracellular bacteria. Lastly, 6 ml of complete DMEM (J774), or DMEM supplemented with 10 ng/ml M-CSF (BMDMs), was added to each flask. Cells were either immediately processed or incubated for further 20 hours. Infections were done in triplicate.

Intracellular survival and growth was assessed by lysis of the monolayers by the addition of 0.1% Triton X-100 in DPBS and enumeration of bacteria by serial dilution in PBS-T plating onto Middlebrook 7H11 solid medium. Colonies were counted after 3–4 weeks incubation at 37°C and the average CFU/ml determined.

RNA extraction. Macrophages were lysed by adding 4 M GTC solution (4 M guanidine thiocyanate, 0.5% sodium N-Lauroylsarcosine, 0.1 M β -mercaptoethanol, 0.5% Tween 80), and the lysate homogenized using a QIAshredder column (Qiagen). RNA was extracted by BCP phase partitioning and isopropanol precipitation, cleaned with 75% ethanol and treated with Turbo DNase (Ambion, Life Technologies). DNA contamination was checked by PCR using primers for the RNA polymerase II gene *Rpb2* (*Rpb2_Up*: 5' CTATAACCTGAATGTAGCAAGC 3', *Rpb2_Lw*: 5' CCCAATGAGGTGCTAGACTC 3'). The RNA was further cleaned using an RNeasy MinElute Cleanup kit (Qiagen), and its quality and quantity were determined using a Bioanalyzer (Agilent) and Qubit® RNA HS kit (Invitrogen), respectively.

Strand-specific RNA-seq library preparation and sequencing. Approximately 500 ng of RNA from each sample was used to prepare individually barcoded strand-specific RNA-seq libraries. rRNA and mitochondrial RNA was removed using Ribo-Zero Gold Removal Magnetic Kit for human/mouse/rat (Epicentre, now Illumina) following the manufacturer's instructions. mRNA was purified using Agencourt RNAClean XP kit. Libraries were constructed using ScriptSeq™ Complete Kit (Epicentre, now Illumina) as per manufacturer's instructions. Quality and quantity of the libraries were determined using a Bioanalyzer (Agilent) and Qubit® (Invitrogen), respectively. Libraries were then quantified by qPCR in an Applied Biosystems® 7500 with the Kapa Biosystems kit for library quantitation (Kapa Biosystems). Next-generation sequencing was performed using an Illumina HiSeq 2000 flow cell with one 150-bp end run. The NCBI Gene Expression Omnibus (GEO) accession number for the RNA-seq data reported in this paper is GSE88801.

RNA-seq data analysis. Reads were aligned versus the Ensembl mouse genome version mm10 (GRCm38) using STAR⁷⁵ 2.4.2a (Parameters: –outFilterMultimapNmax 20 –lnIntronMax 1000000 –alnSJoverhangMin 8 –alnSJDBoverhangMin 1). Uniquely aligned reads in BAM format were annotated against the protein-coding mRNA regions using SeqMonk v.0.33.1 platform (Babraham Bioinformatics, Cambridge UK). A median of 39.7 (31.7–59.3) and 51.3 (20.1–78.4) million single-end reads per library were obtained for the BMDMs and J774 libraries, respectively (Supplementary Data S5). Of these, a median of 82.47% (78.86–85.87%) and 78.93% (69.63–84.09%) of the reads mapped to unique locations in the *Mus musculus* reference genome (Supplementary Data S5, Figure S4), with a median of 92.25% (73.80–96.75%) and 93.88% (70.67–96.55%) assigned to genes (Supplementary Data S5, Figure S5). Contamination with rRNA or mitochondrial DNA was very low at a median of only 0.28% (0.15–4.47%) and 1.26% (0.95–5.34%), respectively, for the BMDMs libraries, and a 1.12% (0.07–4.69%) and 1.98% (0.71–5.28%) for the J774 libraries (Supplementary Data S5, Figure S5). Differential expression was analysed in SeqMonk after quantification of raw counts, strand-specific, merged isoforms, using the R (version 3.2.2) package DESeq2. A gene was classified as up- or downregulated using a cut-off value of more or less than 2-fold expression difference, with an adjusted *P*-value < 0.05, following multiple testing correction. DEGs were further analysed using QIAGEN's Ingenuity® Pathway Analysis (IPA®, QIAGEN) to identify over-represented canonical pathways.

References

- Rajaram, M. V., Ni, B., Dodd, C. E. & Schlesinger, L. S. Macrophage immunoregulatory pathways in tuberculosis. *Semin Immunol* **26**, 471–485 (2014).
- Dey, B. & Bishai, W. R. Crosstalk between Mycobacterium tuberculosis and the host cell. *Semin Immunol* **26**, 486–496 (2014).
- Cadena, A. M., Flynn, J. L. & Fortune, S. M. The Importance of First Impressions: Early Events in Mycobacterium tuberculosis Infection Influence Outcome. *MBio* **7** (2016).
- Johnson, B. K. & Abramovitch, R. B. Macrophage infection models for Mycobacterium tuberculosis. *Methods Mol Biol* **1285**, 329–341 (2015).
- Mendoza-Corral, E. & Castanon-Arreola, M. Comparative evaluation of *in vitro* human macrophage models for mycobacterial infection study. *Pathog Dis* **74**, ftw052 (2016).
- Burdall, S. E., Hanby, A. M., Lansdown, M. R. J. & Speirs, V. Breast cancer cell lines: friend or foe? *Breast Cancer Research* **5**, 89–95 (2003).
- Pan, C., Kumar, C., Bohl, S., Klingmueller, U. & Mann, M. Comparative proteomic phenotyping of cell lines and primary cells to assess preservation of cell type-specific functions. *Molecular & cellular proteomics: MCP* **8**, 443–450 (2009).
- Frattini, A. *et al.* High variability of genomic instability and gene expression profiling in different HeLa clones. *Scientific Reports* **5**, 15377 (2015).
- Jordao, L., Bleck, C. K., Mayorga, L., Griffiths, G. & Anes, E. On the killing of mycobacteria by macrophages. *Cell Microbiol* **10**, 529–548 (2008).
- Mehta, P. K., King, C. H., White, E. H., Murtagh, J. J. Jr. & Quinn, F. D. Comparison of *in vitro* models for the study of Mycobacterium tuberculosis invasion and intracellular replication. *Infect Immun* **64**, 2673–2679 (1996).
- Dillon, L. A., Suresh, R., Okrah, K., Corrada Bravo, H., Mosser, D. M. & El-Sayed, N. M. Simultaneous transcriptional profiling of *Leishmania major* and its murine macrophage host cell reveals insights into host-pathogen interactions. *BMC Genomics* **16**, 1108 (2015).
- Fernandes, M. C., Dillon, L. A., Belew, A. T., Bravo, H. C., Mosser, D. M. & El-Sayed, N. M. Dual transcriptome profiling of *Leishmania*-infected human macrophages reveals distinct reprogramming signatures. *mBio* **7**, e00027–16 (2016).
- Klug-Micu, G. M. *et al.* CD40 ligand and interferon-gamma induce an antimicrobial response against Mycobacterium tuberculosis in human monocytes. *Immunology* **139**, 121–128 (2013).
- Singh, S. B. *et al.* Human IRGM regulates autophagy and cell-autonomous immunity functions through mitochondria. *Nat Cell Biol* **12**, 1154–1165 (2010).
- Kim, B. H. *et al.* A family of IFN-gamma-inducible 65-kD GTPases protects against bacterial infection. *Science* **332**, 717–721 (2011).
- Bogunovic, D. *et al.* Mycobacterial disease and impaired IFN-gamma immunity in humans with inherited ISG15 deficiency. *Science* **337**, 1684–1688 (2012).
- Michelucci, A. *et al.* Immune-responsive gene 1 protein links metabolism to immunity by catalyzing itaconic acid production. *Proc Natl Acad Sci USA* **110**, 7820–7825 (2013).
- Hall, C. J. *et al.* Immunoresponsive gene 1 augments bactericidal activity of macrophage-lineage cells by regulating beta-oxidation-dependent mitochondrial ROS production. *Cell Metab* **18**, 265–278 (2013).
- Roca, F. J. & Ramakrishnan, L. TNF dually mediates resistance and susceptibility to mycobacteria via mitochondrial reactive oxygen species. *Cell* **153**, 521–534 (2013).
- Krishnan, N., Robertson, B. D. & Thwaites, G. Pathways of IL-1beta secretion by macrophages infected with clinical Mycobacterium tuberculosis strains. *Tuberculosis (Edinb)* **93**, 538–547 (2013).
- Jayaraman, P. *et al.* IL-1beta promotes antimicrobial immunity in macrophages by regulating TNFR signaling and caspase-3 activation. *J Immunol* **190**, 4196–4204 (2013).
- Fantuzzi, G. & Dinarello, C. A. Interleukin-18 and interleukin-1 beta: two cytokine substrates for ICE (caspase-1). *J Clin Immunol* **19**, 1–11 (1999).
- Volkman, H. E. *et al.* Tuberculous granuloma induction via interaction of a bacterial secreted protein with host epithelium. *Science* **327**, 466–469 (2010).
- Vesosky, B., Rottinghaus, E. K., Stromberg, P., Turner, J. & Beamer, G. CCL5 participates in early protection against Mycobacterium tuberculosis. *J Leukoc Biol* **87**, 1153–1165 (2010).
- Diamond, M. S. IFIT1: A dual sensor and effector molecule that detects non-2'-O methylated viral RNA and inhibits its translation. *Cytokine & growth factor reviews* **25**, 543–550 (2014).
- Haller, O., Staeheli, P., Schwemmle, M. & Kochs, G. Mx GTPases: dynamin-like antiviral machines of innate immunity. *Trends in microbiology* **23**, 154–163 (2015).
- Helbig, K. J. & Beard, M. R. The role of viperin in the innate antiviral response. *Journal of molecular biology* **426**, 1210–1219 (2014).
- Khounlotham, M., Subbian, S., Smith, R., 3rd, Cirillo, S. L. & Cirillo, J. D. Mycobacterium tuberculosis interferes with the response to infection by inducing the host EphA2 receptor. *J Infect Dis* **199**, 1797–1806 (2009).
- Jager, E. *et al.* Dendritic Cells Regulate GPR34 through Mitogenic Signals and Undergo Apoptosis in Its Absence. *J Immunol* **196**, 2504–2513 (2016).
- Liebscher, I. *et al.* Altered immune response in mice deficient for the G protein-coupled receptor GPR34. *J Biol Chem* **286**, 2101–2110 (2011).
- Arts, R. J., Joosten, L. A., van der Meer, J. W. & Netea, M. G. TREM-1: intracellular signaling pathways and interaction with pattern recognition receptors. *J Leukoc Biol* **93**, 209–215 (2013).
- Wu, M. *et al.* TREM-1 amplifies corneal inflammation after *Pseudomonas aeruginosa* infection by modulating Toll-like receptor signaling and Th1/Th2-type immune responses. *Infect Immun* **79**, 2709–2716 (2011).
- Sathyamoorthy, T. *et al.* Membrane Type 1 Matrix Metalloproteinase Regulates Monocyte Migration and Collagen Destruction in Tuberculosis. *J Immunol* **195**, 882–891 (2015).
- Schroder, W. A. *et al.* A physiological function of inflammation-associated SerpinB2 is regulation of adaptive immunity. *J Immunol* **184**, 2663–2670 (2010).
- Bufé, B. *et al.* Recognition of bacterial signal peptides by mammalian formyl peptide receptors: a new mechanism for sensing pathogens. *J Biol Chem* **290**, 7369–7387 (2015).
- Hu, X. *et al.* Integrated regulation of Toll-like receptor responses by Notch and interferon-gamma pathways. *Immunity* **29**, 691–703 (2008).
- Strick, D. J. & Elferink, L. A. Rab15 effector protein: a novel protein for receptor recycling from the endocytic recycling compartment. *Mol Biol Cell* **16**, 5699–5709 (2005).
- Zuk, P. A. & Elferink, L. A. Rab15 differentially regulates early endocytic trafficking. *J Biol Chem* **275**, 26754–26764 (2000).
- Kruidenier, L. *et al.* A selective jumonji H3K27 demethylase inhibitor modulates the proinflammatory macrophage response. *Nature* **488**, 404–408 (2012).
- Holla, S. *et al.* MUSASHI-Mediated Expression of JMJD3, a H3K27me3 Demethylase, Is Involved in Foamy Macrophage Generation during Mycobacterial Infection. *PLoS Pathog* **12**, e1005814 (2016).
- Khader, S. A. *et al.* IL-23 is required for long-term control of Mycobacterium tuberculosis and B cell follicle formation in the infected lung. *J Immunol* **187**, 5402–5407 (2011).

42. Koo, M. S., Subbian, S. & Kaplan, G. Strain specific transcriptional response in *Mycobacterium tuberculosis* infected macrophages. *Cell Commun Signal* **10**, 2 (2012).
43. Blischak, J. D., Tailleux, L., Mitrano, A., Barreiro, L. B. & Gilad, Y. Mycobacterial infection induces a specific human innate immune response. *Sci Rep* **5**, 16882 (2015).
44. Nalpas, N. C. *et al.* RNA sequencing provides exquisite insight into the manipulation of the alveolar macrophage by tubercle bacilli. *Sci Rep* **5**, 13629 (2015).
45. Tailleux, L. *et al.* Probing host pathogen cross-talk by transcriptional profiling of both *Mycobacterium tuberculosis* and infected human dendritic cells and macrophages. *PLoS One* **3**, e1403 (2008).
46. Hoffmann, R., Van Erp, K., Trülzsch, K. & Heesemann, J. Transcriptional responses of murine macrophages to infection with *Yersinia enterocolitica*. *Cellular Microbiology* **6**, 377–390 (2004).
47. van Erp, K., Dach, K., Koch, I., Heesemann, J. & Hoffmann, R. div xmlns=http://www.w3.org/1999/xhtml Role of strain differences on host resistance and the transcriptional response of macrophages to infection with *Yersinia enterocolitica* /div>. *Physiological Genomics* **25**, 75–84 (2006).
48. Jung, Y. J., Ryan, L., LaCourse, R. & North, Robert J. Differences in the Ability to Generate Type 1 T Helper Cells Need Not Determine Differences in the Ability to Resist *Mycobacterium tuberculosis* Infection among Mouse Strains. *Journal of Infectious Diseases* **199**, 1790–1796 (2009).
49. Wakeham, J., Wang, J. & Xing, Z. Genetically Determined Disparate Innate and Adaptive Cell-Mediated Immune Responses to Pulmonary *Mycobacterium bovis* BCG Infection in C57BL/6 and BALB/c Mice. *Infection and Immunity* **68**, 6946–6953 (2000).
50. Beamer, G. L. & Turner, J. Murine models of susceptibility to tuberculosis. *Arch Immunol Ther Exp (Warsz)* **53**, 469–483 (2005).
51. Garcia-Pelayo, M. C., Bachy, V. S., Kavesh, D. A. & Hogarth, P. J. BALB/c mice display more enhanced BCG vaccine induced Th1 and Th17 response than C57BL/6 mice but have equivalent protection. *Tuberculosis* **95**, 48–53 (2015).
52. Keller, C., Lauber, J., Blumenthal, A., Buer, J. & Ehlers, S. Resistance and susceptibility to tuberculosis analysed at the transcriptome level: lessons from mouse macrophages. *Tuberculosis (Edinb)* **84**, 144–158 (2004).
53. Lee, H.-J., Ko, H.-J. & Jung, Y.-J. Insufficient Generation of Mycobactericidal Mediators and Inadequate Level of Phagosomal Maturation Are Related with Susceptibility to Virulent *Mycobacterium tuberculosis* Infection in Mouse Macrophages. *Frontiers in Microbiology* **7** (2016).
54. Hommes, T. J. *et al.* Triggering receptor expressed on myeloid cells-1 (TREM-1) improves host defence in pneumococcal pneumonia. *J Pathol* **233**, 357–367 (2014).
55. Hommes, T. J. *et al.* Role of triggering receptor expressed on myeloid cells-1/3 in Klebsiella-derived pneumosepsis. *Am J Respir Cell Mol Biol* **53**, 647–655 (2015).
56. Yang, C. *et al.* TREM-1 signaling promotes host defense during the early stage of infection with highly pathogenic *Streptococcus suis*. *Infect Immun* **83**, 3293–3301 (2015).
57. Joosten, S. A., Fletcher, H. A. & Ottenhoff, T. H. A helicopter perspective on TB biomarkers: pathway and process based analysis of gene expression data provides new insight into TB pathogenesis. *PLoS One* **8**, e73230 (2013).
58. Rajaram, M. V. *et al.* *Mycobacterium tuberculosis* activates human macrophage peroxisome proliferator-activated receptor gamma linking mannose receptor recognition to regulation of immune responses. *J Immunol* **185**, 929–942 (2010).
59. Pethe, K. *et al.* Isolation of *Mycobacterium tuberculosis* mutants defective in the arrest of phagosome maturation. *Proc Natl Acad Sci USA* **101**, 13642–13647 (2004).
60. Homolka, S., Niemann, S., Russell, D. G. & Rohde, K. H. Functional genetic diversity among *Mycobacterium tuberculosis* complex clinical isolates: delineation of conserved core and lineage-specific transcriptomes during intracellular survival. *PLoS Pathog* **6**, e1000988 (2010).
61. Rohde, K. H., Veiga, D. F., Caldwell, S., Balazsi, G. & Russell, D. G. Linking the transcriptional profiles and the physiological states of *Mycobacterium tuberculosis* during an extended intracellular infection. *PLoS Pathog* **8**, e1002769 (2012).
62. Ahmadian, M. *et al.* PPARgamma signaling and metabolism: the good, the bad and the future. *Nat Med* **19**, 557–566 (2013).
63. Pizzol, D. *et al.* Tuberculosis and diabetes: current state and future perspectives. *Tropical medicine & international health: TM & IH* **21**, 694–702 (2016).
64. Martinez, N., Ketheesan, N., West, K., Vallerstog, T. & Kornfeld, H. Impaired Recognition of *Mycobacterium tuberculosis* by Alveolar Macrophages from Diabetic Mice. *J Infect Dis* (2016).
65. Lachmandas, E. *et al.* Diabetes Mellitus and Increased Tuberculosis Susceptibility: The Role of Short-Chain Fatty Acids. *Journal of diabetes research* **2016**, 6014631 (2016).
66. Simeone, R. *et al.* Phagosomal rupture by *Mycobacterium tuberculosis* results in toxicity and host cell death. *PLoS Pathog* **8**, e1002507 (2012).
67. Dey, B. *et al.* A bacterial cyclic dinucleotide activates the cytosolic surveillance pathway and mediates innate resistance to tuberculosis. *Nat Med* **21**, 401–406 (2015).
68. Wassermann, R. *et al.* *Mycobacterium tuberculosis* Differentially Activates cGAS- and Inflammasome-Dependent Intracellular Immune Responses through ESX-1. *Cell Host Microbe* **17**, 799–810 (2015).
69. Eigenbrod, T. & Dalpke, A. H. Bacterial RNA: An Underestimated Stimulus for Innate Immune Responses. *The Journal of Immunology* **195**, 411–418 (2015).
70. Patel, J. R. & García-Sastre, A. Activation and regulation of pathogen sensor RIG-I. *Cytokine & growth factor reviews* **25**, 513–523 (2014).
71. Secanella-Fandos, S., Noguera-Ortega, E., Olivares, F., Luquin, M. & Julian, E. Killed but metabolically active *Mycobacterium bovis* bacillus Calmette-Guerin retains the antitumor ability of live bacillus Calmette-Guerin. *The Journal of urology* **191**, 1422–1428 (2014).
72. Datta, S. K. *et al.* Vaccination with irradiated *Listeria* induces protective T cell immunity. *Immunity* **25**, 143–152 (2006).
73. Magnani, D. M., Harms, J. S., Durward, M. A. & Splitter, G. A. Nondividing but metabolically active gamma-irradiated *Brucella melitensis* is protective against virulent *B. melitensis* challenge in mice. *Infect Immun* **77**, 5181–5189 (2009).
74. Bauler, T. J., Chase, J. C., Wehrly, T. D. & Bosio, C. M. Virulent *Francisella tularensis* destabilize host mRNA to rapidly suppress inflammation. *J Innate Immun* **6**, 793–805 (2014).
75. Dobin, A. *et al.* STAR: ultrafast universal RNA-seq aligner. *Bioinformatics* **29**, 15–21 (2013).

Acknowledgements

T.G.C is supported by the Medical Research Council UK (Grant no. MR/K000551/1, MR/M01360X/1, MR/N010469/1, MC_PC_15103). Sequence analysis was performed on the MRC UK funded eMedlab computing resource.

Author Contributions

N.A. and M.L.H. conceived the project and designed the experiments. N.A. and P.F.S. conducted the experiments. N.A., J.P., P.F.S., J.M.C., T.C., and M.L.H. analysed the results. N.A. wrote the paper. All authors reviewed the paper.

Additional Information

Supplementary information accompanies this paper at <http://www.nature.com/srep>

Competing financial interests: The authors declare no competing financial interests.

How to cite this article: Andreu, N. *et al.* Primary macrophages and J774 cells respond differently to infection with *Mycobacterium tuberculosis*. *Sci. Rep.* 7, 42225; doi: 10.1038/srep42225 (2017).

Publisher's note: Springer Nature remains neutral with regard to jurisdictional claims in published maps and institutional affiliations.



This work is licensed under a Creative Commons Attribution 4.0 International License. The images or other third party material in this article are included in the article's Creative Commons license, unless indicated otherwise in the credit line; if the material is not included under the Creative Commons license, users will need to obtain permission from the license holder to reproduce the material. To view a copy of this license, visit <http://creativecommons.org/licenses/by/4.0/>

© The Author(s) 2017